Physical investigation of $In_2O_3:Sn$ thin films fabricated by chemical spray pyrolysis

Salam Amir Yousif, Duha Ismail Khalil

Salammomica@yahoo.com,

Abstract

$In_2O_3:Sn$ (ITO) thin films were deposited for various Tin concentrations (0, 5, 10, 15, 20) % on glass substrates at substrate temperature equal to (450 ± 10)℃ using the simple flexible and cost-effective spray pyrolysis technique. The structural and optical properties of these films have been investigated. The structure of the samples are polycrystalline with a cubic lattice crystal structure and the preferred growth way in the (400) trend. The optical properties of indium tin oxide thin films have been studied from the transmission and absorption spectrum in the wavelength interval from (300 - 1000) nm. The transmittance, optical band gap and Urbach energies of tin doped indium oxide have been investigated.

***Keywords*:** In_2O_3; X-ray Diffraction; Optical Characterization.

أ.م.د سلام أمير يوسف ضحى اسماعيل خليل

قسم الفيزياء، كلية التربية، الجامعة المستنصرية، بغداد، العراق

الخلاصة

تم ترسيب اغشية اوكسيد الانديوم المشوبة بالقصدير بتراكيز مختلفة % (0, 5, 10, 15, 20) على قواعد زجاجيه وبدرجة حرارة (450 ± 10)℃ بواسطة تقنية التحلل الكيميائي الحراري. تم التحقق من الخصائص التركيبية والبصرية لهذه الاغشية اذ اظهرت نتائج حيود الاشعة السينية بان الاغشية المحضرة ذات تركيب مكعب متعدد التبلور وباتجاه سائد (400). تم دراسة الخصائص البصرية للأغشية الرقيقة بوساطة طيف النفاذية عند درجة حرارة الغرفة ولمدى الاطوال الموجية من

nm (300−1000). تم حساب النفاذية وفجوة الطاقة وطاقات اورباخ لأغشية اوكسيد الانديوم المشوبة بالقصدير.

1- Introduction

Transparent conducting oxides (TCO) possess n-type like indium tin oxide, In_2O_3: Sn (ITO), antimony or fluorine doped tin oxide; SnO_2: Sb (ATO) and SnO_2: F (FTO) are particularly attractive. They find many applications in order to of optical band gap energy Eg of typically (3.5 <Eg< 4.0) ev. Characteristic in necessary in order to have materials there are very transparent in visible range (more than 80% depending on thickness and the deposition technique) and high electrical conductivity conductivity (about $10^3(\Omega.cm)^{-1}$ or more) and high reflectance in the infrared (IR) region. Their resistivity could be as low as ($10^{-4}\Omega$.cm). Indeed in materials with Eg $3ev$ the visible light energy hv ($1.65ev$ < hv < $3.26ev$) is insufficient to be absorbed by band-to-band electron transition mechanism this is achieved in TCO by incorporating extrinsic dopant elements in the crystalline network or by either crystal defects. One advantage of using binary TCO materials is that the control of chemical in film deposition is relatively easier than in ternary compounds ($GaInO_3$, $Zn_2In_2O_5$, . . .) and multicomponent oxides ($ZnO–In_2O_3$, $ZnO–SnO_2$, . . .) [1-5]. In_2O_3 is a wide band gap (direct band gap energy of (3.4-3.75)ev Transparent conducting semiconductor possessing cubic structure with lattice parameters, a = b = c = 10.18 Å [6, 7]. Among the different transparent conducting oxides, indium oxide has attracted enormous attention due to its tremendous applications in many fields. It is applied in thin film infrared reflectors transparent for visible light (hot mirrors), antireflection coatings, electroluminescent devices, electrochromic devices, photothermal devices, photocatalyst sensors, light emitting diodes, some

types of batteries, resistive elements and integrated circuits. It can also be used in optoelectronic devices, thin film solar cells and photo detectors, gas sensors [8,9]. Thin films of indium oxide can be prepared by a variety of techniques such as chemical vapor deposition, spray pyrolysis, chemical vapor deposition, magnetron sputtering and vacuum evaporation. Spray pyrolysis offers deposition of thin films with low cost, easily modified to mass production [(10-14)].

Experimental part

ITO thin films with various Tin-doping (0, 5, 10, 15, 20) %, were prepared on glass substrates by spray pyrolysis (SP) technique. The pure Indium Chloride $InCl_3$, pure Stannic Chloride $SnCl_4.5H_2O$ and distilled water were blended to obtain a solution with 0.05M concentration. In this work the deposition conditions are; substrate temperature (450 ± 10)℃, gas pressure $(3\ bar)$, carrier gas Nitrogen (N_2) under ambient atmosphere, spraying rate $(5-6\ ml/\text{min})$, concentration of solution $(0.05\ Molarity)$, the spraying time period is 8 *sec* with 80 *sec* wait between the steps of spraying, and the nozzle distance from the substrate equal to 30 *cm*. The x-ray diffraction instrument type (Shimadzu 6000) was used to investigate the structural properties of ITO thin films. Optical calculations of the ITO thin films have been measured using Shimadzu (UV-1650 PC) spectrophotometer in the wavelength interval between 300 to 1000 nm by analysis of transmitted and absorbed beams.

3- Results and discussion

3-1 Structural results

X- ray diffraction pattern of indium oxide thin films have been shown in figure (1). The peaks of XRD were observed between 10^0 and 80^0. The presence of diffraction peaks indicates that the film is polycrystalline with

cubic crystal structure and no amorphous phase is detected. It is revealed that the sprayed film has peaks corresponding to (211), (222), (400), (440) and (622) directions of the cubic In_2O_3 crystal structure which is corresponding to the position $2\theta = (21.3989^0, 30.4776^0, 35.36^0, 50.9178^0)$ and (60.5847^0) respectively. The XRD measurements revealed that the In_2O_3 film shows a peak (400) which have higher intensity with a texture coefficient equal to 2.8418 as a preferred growth orientation, which is in agreement with Joint Committee of Powder Diffraction Standard (JCPDS) card file data. The presence of other peaks such as (211), (222), (444) and (622) have also been detected but with substantially low intensities.

The interplanar spacing of (400) plane of the In_2O_3 thin film was evaluated for the position of (400) peak from the XRD data. The observed d value is 2.53638Å which is in agreement with the standard value 2.529 Å taken from the (JCPDS) and the position of (400) peak taken from the XRD pattern is 35.36^0 which is in agreement with the standard value 35.4657^0 taken from (JCPDS). The observed d-values are presented in Table (1) and compare with the standard ones from the (JCPDS) values. The matching of the observed and standard d-values confirms that the deposited films are of indium oxide with cubic structure.

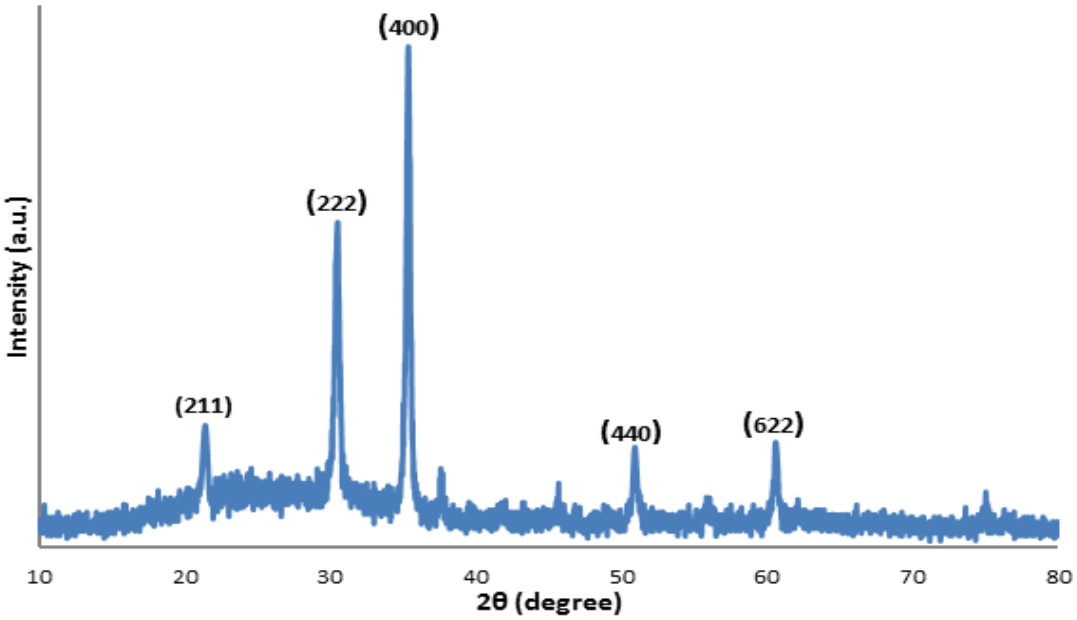

Fig. 1: XRD pattern of pure In_2O_3 film

Figure [2-5] illustrates x-ray diffraction forms of $In_2O_3{:}Sn$ samples which having tin-content equal to (5, 10, 15, 20) %. The x-ray diffraction spectra of $In_2O_3{:}Sn$ films for different tin doping levels in the precursor solution show that the films are polycrystalline with cubic crystal structure with no amorphous phases. These films have peaks corresponding to (211), (222), (400), (440) and (622) directions of the cubic In_2O_3 crystal structure. It is evident from the XRD spectra that no diffraction peaks of Sn or other impurity phases are detected in the prepared samples. XRD patterns show that the doped films have the peak (222) as the highest intensity. Other binary peaks have been observed with lowest intensities like (211), (400), (440) and (622) in the XRD forms. All XRD patterns show that the intensity of (222) peak increase with adding Tin-content in the samples, and the intensity of (400) peak decrease with adding Tin-content in the samples as shown in figures [1-5]. Due to the replacement of smaller radius Sn^{4+} ion (0.71 Å) in indium sites and also related to changes of strain in the crystal lattice, which is in agreement with the report [15].

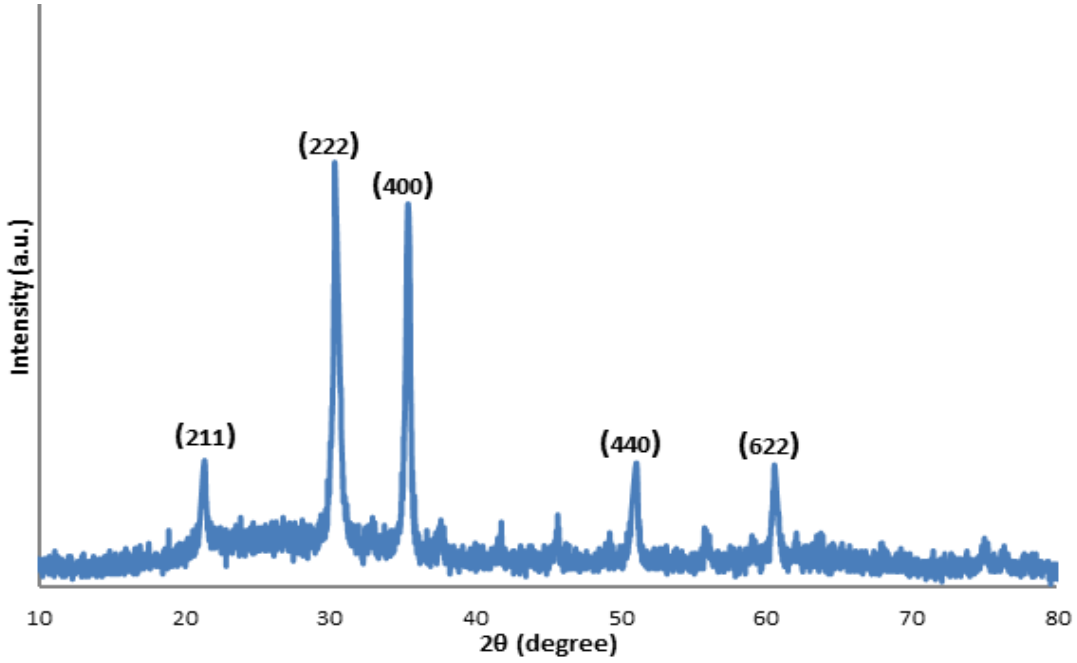

Fig.2: XRD pattern of In_2O_3: Sn film (Sn=5%)

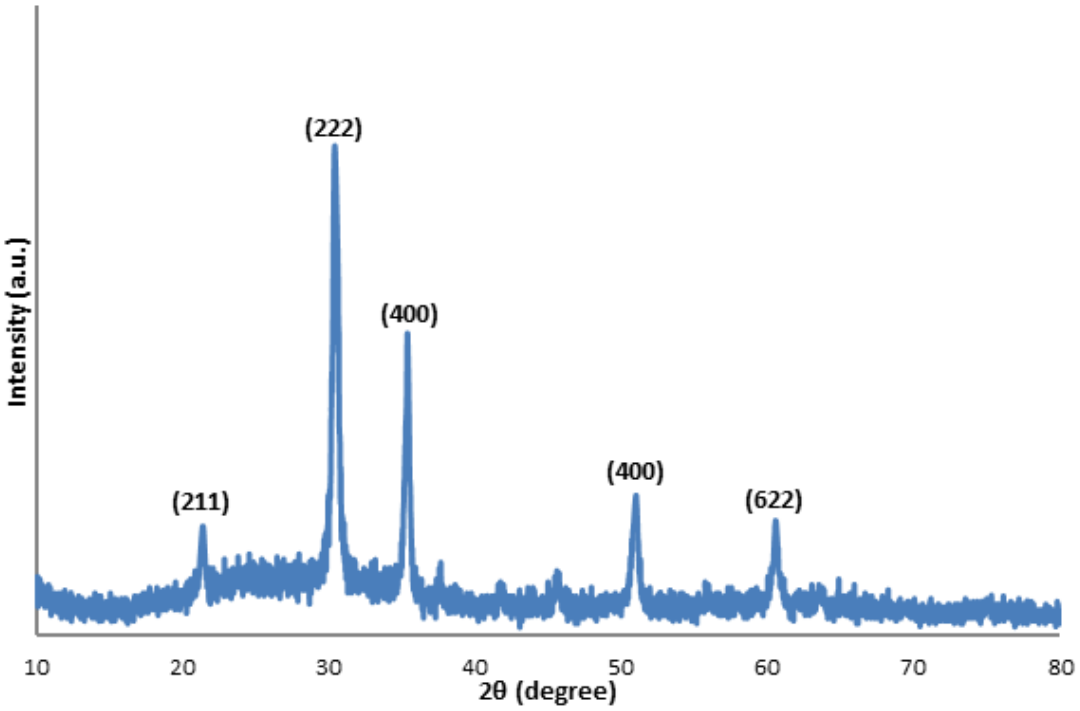

Fig.3: XRD pattern of In_2O_3: Sn film (Sn=10%)

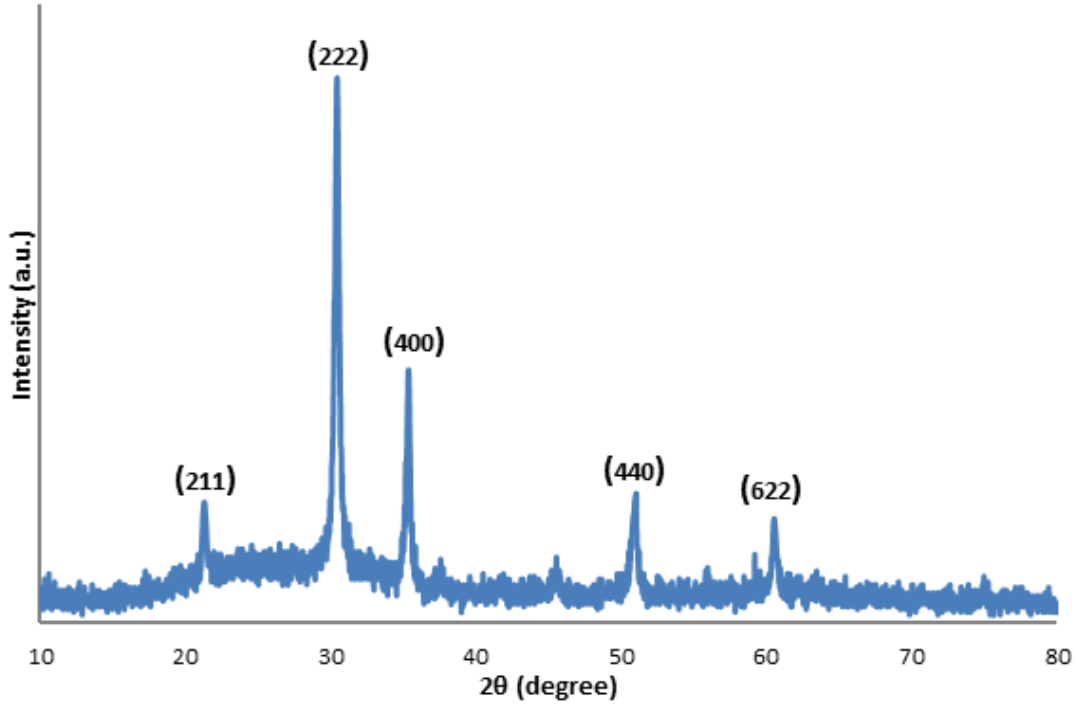

Fig.4: XRD pattern of $In_2O_3:Sn$ film (Sn=15%)

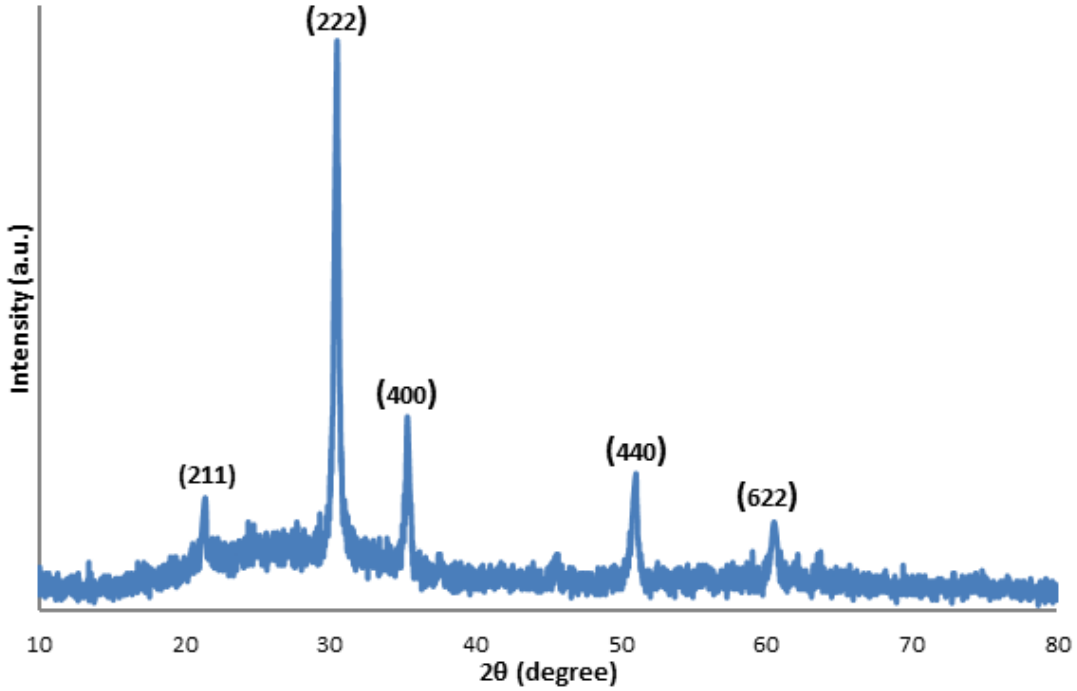

Fig.5: XRD pattern of $In_2O_3:Sn$ film (Sn=20%)

Table 1: XRD analysis of ($In_2O_3:Sn$) films.

Sn- content %			0	5	10	15	20	ASTM for In_2O_3
hkl	211	2θ(deg)	21.3989	21.4214	21.3989	21.3491	21.4089	21.4982
		d(Å)	4.14904	4.14474	4.14904	4.15861	4.14713	4.130000
		Int.	11	13	11	10	9	14
	222	2θ(deg)	30.4776	30.5074	30.4575	30.4318	30.4855	30.5799
		d(Å)	2.93065	2.92786	2.93254	2.93496	2.92991	2.921000
		Int.	62	100	100	100	100	100
	400	2θ(deg)	35.3600	35.3934	35.3609	35.3274	35.3699	35.4657
		d(Å)	2.53638	2.53406	2.53632	2.53865	2.53569	2.529000
		Int.	100	79	48	47	30	30
	440	2θ(deg)	50.9178	50.9544	50.9298	50.8811	50.9303	51.0374
		d(Å)	1.79196	1.79076	1.79157	1.79317	1.79155	1.788000
		Int.	17	23	25	24	22	35
	622	2θ(deg)	60.5847	60.5982	60.5416	60.5172	60.5366	60.6762
		d(Å)	1.52712	1.52682	1.52811	1.52867	1.52822	1.525000
		Int.	16	21	17	14	12	25

The lattice distance (a) of $In_2O_3:Sn$ thin films deposited on glass substrate at different tin doping (0, 5, 10, 15, 20) % by spray pyrolysis (SP) technique have been calculated using equation (1)[16]. The lattice constant (a) has been illustrated in Table (2), which are matched with the published and standard values. Figure (6) shows the lattice distance (a) vs. Tin-content.

$$a = d\sqrt{h^2 + k^2 + l^2} \ldots\ldots (1)$$

Table 2: Lattice constants of In_2O_3: Sn thin films of different tin content

Sample	Sn- Concentration (%)	a (Å)
1	0	10.15
2	5	10.14
3	10	10.15
4	15	10.16
5	20	10.14
ASTM	0	10.118

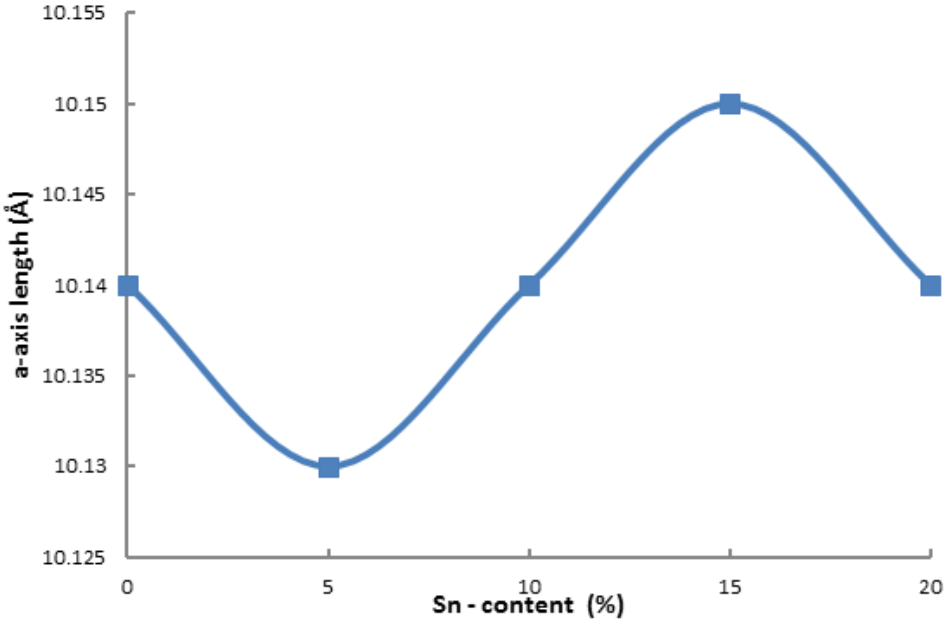

Fig. 6: a-axis length estimated along (400) direction vs. tin doping

The crystallite size (D) is calculated by using Scherrer's formula given by relation (2) [17].

$$\mathbf{D = \frac{K\lambda}{\beta \cos\theta}} \ldots\ldots (2)$$

The value of crystallite size of ITO thin films, along (400) direction as preferred orientation, decreases with increasing Sn- content in the films from (27.6) nm at Sn- doping = 0 % to (23-24) nm at other concentration. It can be noted that the value of crystallite size of ITO thin films is kept constant (23-24) nm approximately for the films prepared at (Sn-doping = 5-20) %. The film prepared at Sn-doping, (Sn=0 %) showed the highest

crystallite size and its value decreases with increasing Sn-doping ratio as shown in Table (3) and Fig.(7). a show The variation in crystallite size arises due to changes in the density of nucleation centers, resulting in the film undergoing compressive stress in the case of smaller crystallite sizes and tensile stress in the case of larger crystallite sizes. The XRD peaks can be widened (increasing of FWHM) by internal stress and defect when increasing Sn-doped in the samples.

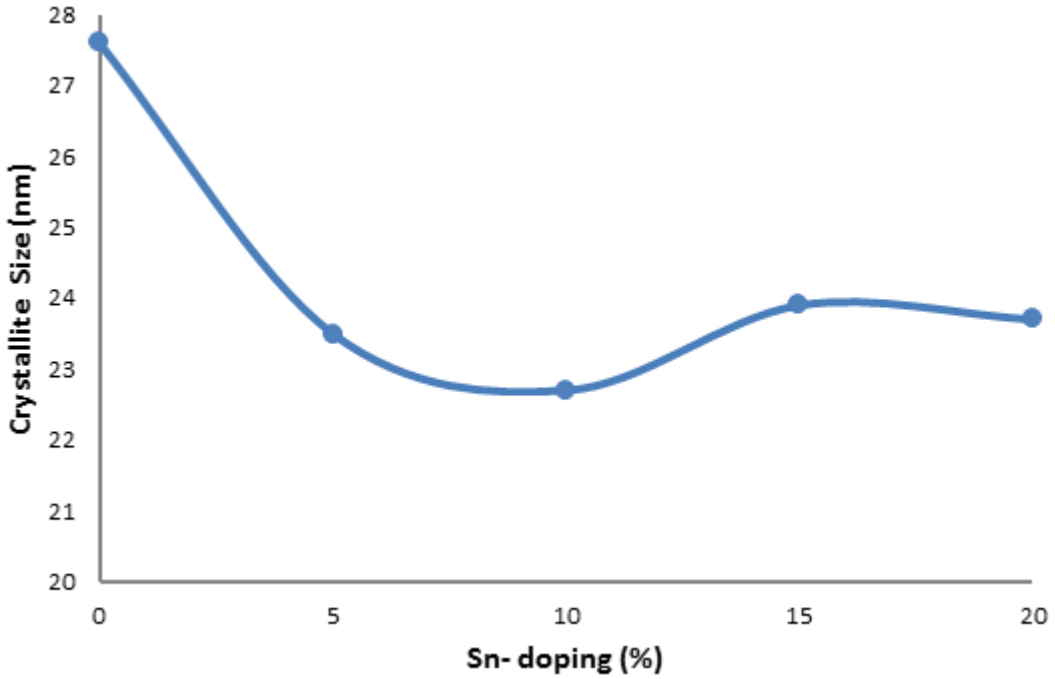

Fig. 7: Crystallite size of (400) direction vs. tin doping

The values of full width at half maximum (FWHM) of the preferred orientation (400) for ITO thin films increase with increasing Sn- content up to (10%), then it goes on decreases with increasing Sn- content at (15, 20)%. Highest value of FWHM of (400) plane has been observed at Sn-doping equal to (10%).

The microstrain (ε) of tin doped indium oxide (ITO) thin films arises from the deposition process on the heated substrate and makes the stretching or compression in the crystal lattice which leads to the deviation

in the distance between the atoms from the standard value. Due to imperfections, impurities, and crystal defects that arose during the time of film growth, strain is produced in the film which, in turn, influences the structural, optical, and transport properties of the film, which is in agreement with the report [18]. This strain can be calculated from the formula given by equation (3), [19] as shown in Table (3).

$$\boldsymbol{\varepsilon = \frac{\beta\, COS\theta}{4}} \ldots\ldots (3)$$

The number of layer (N_ℓ) which could be estimated by due to the percolation theory, and it depends on the film thickness (t) using equation [20] as shown in Table (3). The number of layers varies with Sn- content in the films in random way. It is thought that the quantity of drop and substrate temperature varies play a great role in this random change.

$$\boldsymbol{t = D \times N_l} \ldots\ldots (4)$$

The number of crystallites per unit area ($N_\circ$) is calculated using the equation (5) [21] and listed in Table (3).

$$\boldsymbol{N_\circ = \frac{t}{D^3}} \ldots\ldots (5)$$

The number of crystallites of tin doped indium oxide thin films prepared on glass substrate by spray pyrolysis method at a substrate temperature (450 ± 10)℃ has been calculated from the film thickness and the crystallite size.

To describe the preferential direction, the texture coefficient (TC) is calculated using the following equation (6) [22]

$$\boldsymbol{T_c(hkl) = \frac{I(hkl)/I_0(hkl)}{N_r^{-1} \sum I(hkl)/I_0(hkl)}} \ldots\ldots (6)$$

Where:-

I: is the relative intensity. I_o: is the ASTM relative standard intensity.

N_r: is the number of reflections. hkl: is the Miller indices.

The texture coefficient of ITO thin films estimated along (400) trend has been shown in figure (8) and illustrated in Table (3). The texture coefficient of indium tin oxide thin films along (400) direction decreases with increasing Sn-content in the film. The alteration of preferred growth direction may be due to occupancy of additional indium vacancy sites by tin atoms, which are unoccupied previously. In_2O_3 thin films have several defect levels, such as indium vacancies and indium interstitial oxygen, which is consistent with the research [15].

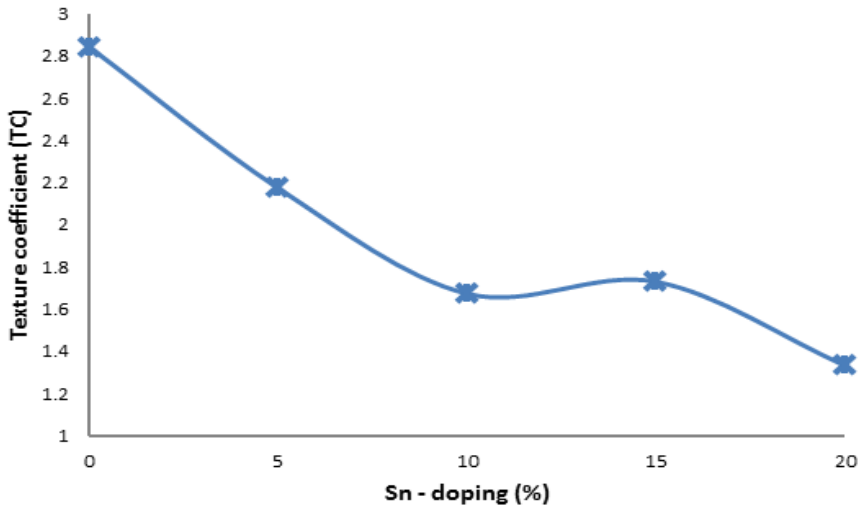

Fig. 8: Texture coefficient estimated along (400) direction vs. tin doping

Table 3: Structural properties of $In_2O_3:Sn$ thin films

Sample	hkl	FWHM (deg)	Crystallite size (nm)	Dislocation Density ,δ (10^15line/m^2)	Strain ,ε x(10^-3)	*Number of crystallite per unit area (N_o) (cry/m2) x10^{18}*	*Number of layer(N_l)*	Lattice Constant(Å)	TC
0 %	211	0.32000	25.2	1.57	1.37	0.04036741	25.63	10.16	0.6698
	222	0.33380	24.6	1.65	1.40	0.043393751	26.26	10.15	0.5285
	400	0.30140	27.6	1.31	1.25	0.03072597	23.40	10.14	2.8418
	440	0.27600	31.8	0.98	1.08	0.020088668	20.31	10.13	0.4140
	622	0.29470	31.2	1.02	1.11	0.021270061	20.70	10.12	0.5456
5 %	211	0.35500	22.7	1.94	1.52	0.053428712	27.53	10.15	0.7662
	222	0.40710	20.2	2.45	1.71	0.075827355	30.94	10.14	0.8252
	400	0.35480	23.5	1.81	1.47	0.048158885	26.59	10.13	2.1730
	440	0.41330	21.2	2.22	1.62	0.065595256	29.48	10.13	0.5422
	622	0.40170	22.9	1.90	1.51	0.052044347	27.29	10.12	0.6931
10 %	211	0.36000	22.4	1.99	1.54	0.055696804	27.94	10.16	0.8218
	222	0.40180	20.4	2.40	1.69	0.073736722	30.68	10.15	1.0460
	400	0.36670	22.7	1.94	1.52	0.053517616	27.57	10.14	1.6736
	440	0.35600	24.7	1.63	1.40	0.041541624	25.34	10.13	0.7471
	622	0.39500	23.2	1.85	1.48	0.050131462	26.98	10.13	0.7112
15 %	211	0.35340	22.8	1.92	1.51	0.045307463	23.55	10.18	0.7889
	222	0.40600	20.2	2.45	1.70	0.065150863	26.58	10.16	1.1045
	400	0.34760	23.9	1.75	1.44	0.039335129	22.46	10.15	1.7304
	440	0.41330	21.2	2.22	1.62	0.056359444	25.33	10.14	0.7574
	622	0.40600	22.6	1.95	1.53	0.046520992	23.76	10.14	0.6185
20 %	211	0.32660	24.7	1.63	1.40	0.041674345	25.42	10.15	0.8568
	222	0.36850	22.3	2.01	1.55	0.056629803	28.16	10.14	1.3328
	400	0.35130	23.7	1.78	1.46	0.047175292	26.49	10.14	1.3328
	440	0.46500	18.9	2.79	1.83	0.093019549	33.22	10.13	0.8377
	622	0.53500	17.1	3.41	2.01	0.125594699	36.72	10.13	0.6397

3-2 Optical results

The optical properties of indium tin oxide thin films prepared at different tin concentrations 0, 5, 10, 15, 20 % on glass substrate at substrate temperature (450 ± 10)℃ by spray pyrolysis technique have been studied by analysis of transmitted and absorbed spectrum in the wavelength interval from (300 - 1000) nm.

The transmittance (T) spectra of $In_2O_3:Sn$ thin films have been shown in figure (9). We can be noted that the transmittance of the $In_2O_3:Sn$ thin films increase with adding tin doping up to Sn = 5 %. Thereafter, it decreases gradually with increasing tin content in Sn = 10, 15, 20 %. The transmittance of ITO thin film at visible region (550 nm) has been found (66, 77, 74, 73, 69) % for the tin doping (0, 5, 10, 15, 20) %. The transmittance value of 84 % for the In_2O_3 film is found to increase to 86 %

for 5wt% of tin doping at a wavelength equal to 1000 nm. When a high impurity is added, the transmittance of ITO thin film will decrease due to increased photon scattered by crystal defects created by impurities [23-25]. The optical characterization depends on the uniformity and roughness of the ITO film surface. When the surface is rough, the light will be scattered by the film surface and the films will be less transparent.

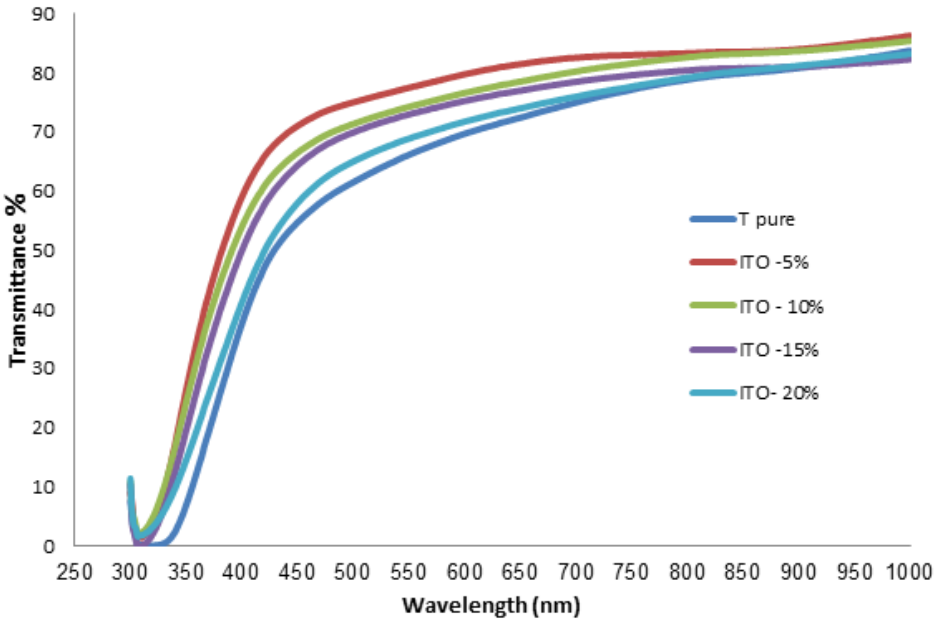

Fig. 9: Transmittance spectra of In_2O_3: Sn films

The optical band gap (Eg) is given by the following relation [26].

$$\alpha h\gamma = A(h\gamma - E_g)^r \ldots\ldots (7)$$

Where:

Eg: optical energy gap of the film. $h\gamma$: incident photon energy.

A: constant. **r**: numeric value equal to (1/2) for allowed direct transition

The fundamental absorption refers to the excitation of an electron from valence band to conduction band (band-to-band transition) and can be used to determine the band gap of material. ITO thin films deposited on glass substrate at substrate temperature (450 ± 10)℃ by spray pyrolysis method have direct allowed transition and the optical band gap have been

calculated from above equation (7). Figure (10) shows the relation between $(h\gamma)$ along x-axis and $(\alpha h\gamma)^2$ along y-axis and the values of direct band gap are estimated from the extrapolated of the linear portion of the curves to zero absorption. The optical band gap of indium tin oxide thin films are found to be (3.5, 3.7, 3.675, 3.65, 3.58) eV corresponds to the Sn-concentration (0, 5, 10, 15, 20) % respectively. The optical band gap of indium tin oxide thin films increase with the increasing of Tin doping from (0 – 5) % because the widening of the band gap is due to the increase in carrier density as a result of Sn-doping and then it increases afterward for further increasing in tin doping from (5 – 20) %. Adding the impurities to the indium oxide films caused the donor levels inside the energy gap near the conduction band; in this case, the incident photon tend be absorbed with low energy compared with the undoped film [27].

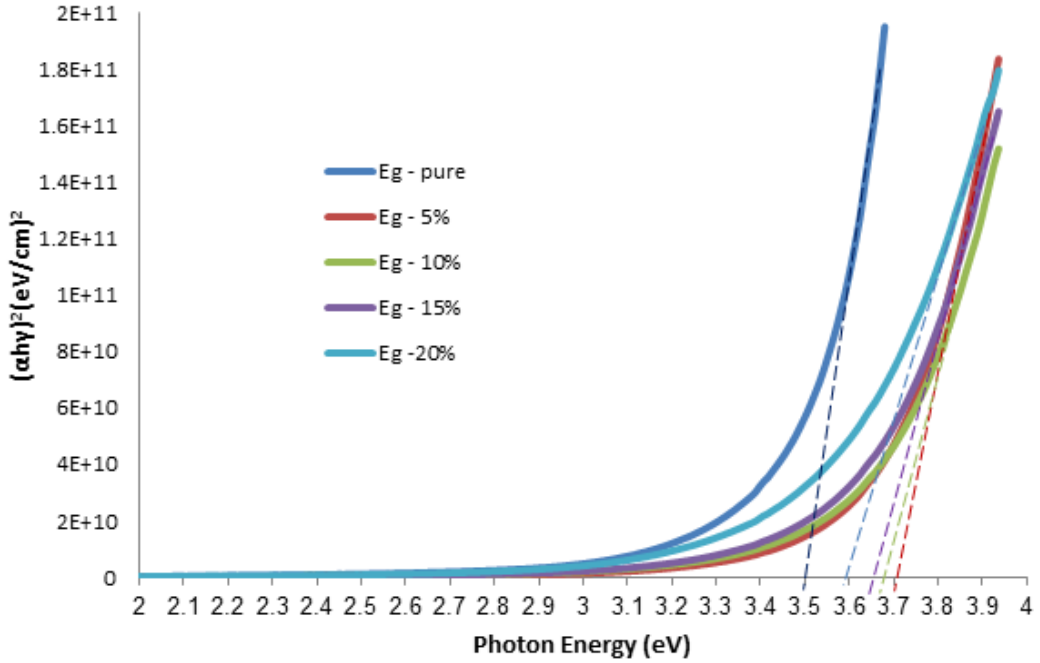

Fig. 10: Optical band gap of $In_2O_3:Sn$ thin films as a function of wavelength for different tin doping

The absorption coefficient near the essential absorption edge is exponentially dependent on the incident photon energy, the Urbach tail expressed by the following equation [8].

$$\alpha = \alpha_0 \exp\left[\frac{h\gamma - E_1}{E_u}\right] \dots\dots (8)$$

Were α_o and E_1 are constants. The width of the exponential curve near the absorption edge represents the Urbach energy E_U. Figure (11) shows Urbach plots of the tin doped indium oxide thin films. The values of Urbach Energy were obtained from the inverse of the slope of *(lnα)* versus *(hγ)* as listed in Table (4). The dopant (Tin) changes the width of the localized states in the optical band, and Urbach Energy values change inversely with optical band gap. Urbach Energy of indium tin oxide thin films decrease with the increasing of tin doping from (0 – 5) % and then it increases afterward for further increasing in tin doping from (5 – 20) % as shown in Table (4).

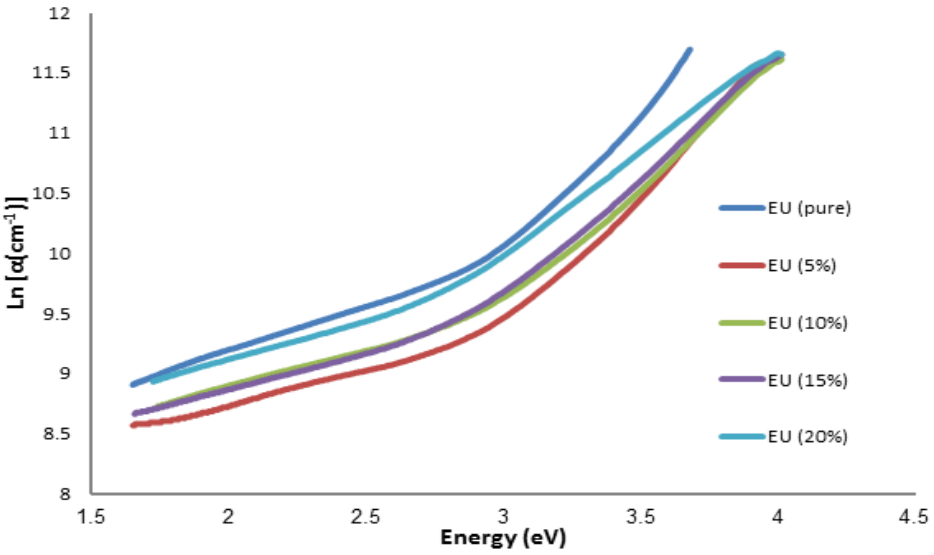

Fig. 11: The Urbach plots of In_2O_3:Sn thin films for different tin doping

Table (4) Optical properties of ITO thin films

Sn-content (%)	E_U (eV)	E_g (eV)	Transmittance (at 550 nm)
0	1.091	3.5	66 %
5	1.074	3.7	77 %
10	1.105	3.675	74 %
15	1.122	3.65	73 %
20	1.129	3.58	69 %

4. Conclusion

Tin doped indium oxide (ITO) thin films were made on glass substrate at heated to $(450 \pm 10)℃$ by chemical spray pyrolysis method. All XRD patterns show that the intensity of (222) peak increase with adding tin - content in the samples, and the intensity of (400) peak decrease with increasing Sn- content in the film, due to the replacement of smaller radius Sn^{4+} ion (0.71 Å) in indium sites and also related to changes of strain in the crystal lattice. We can be noted that the transmittance of the $In_2O_3:Sn$ thin films increase with adding tin-content up to Sn = 5 %. Thereafter, it decreases gradually with increasing tin content at Sn = 10, 15, 20 %. When a high impurity is added, the transmittance of ITO thin film will decrease due to increased photon scattered by crystal defects created by impurities.

References

[1] M. Ait Aouaj , R. Diaz , A. Belayachi , F. Rueda and M. Abd-Lefdil ,"Comparative study of ITO and FTO thin films grown by spray pyrolysis ", Materials Research Bulletin 44 1458–1461 (2009).

[2] Nafiseh Memarian , Seyed Mohammad Rozati , Elangovan Elamurugu and Elvira Fortunato ,"P hys. Status Solidi C 7, No. 9, 2277–2281 (2010).

[3] Je'rôme Steinhauser," Low pressure chemical vapor deposited zinc oxide for silicon thin solar cells ", Lulu.com, (2009).

[4] D. C. Look , J. W. Hemsky and J. R. Rozdove , "Residual native shallow donor in ZnO Phys ",Rev. Lett.,vol. 82, pp. 2552-2555, (1999).

[5] D. C. Look , J. W. Hemsky and J. R. Rozdove , "Residual native shallow donor in ZnO Phys ",Rev. Lett.,vol.82, pp. 2552-2555, (1999).

[6] E. Savarimuthu, K.C. Lalithambik, A. Moses Ezhil Raj, L.C. Nehru, S.Ramamurthy, A. Thayumanavan, C. Sanjeeviraja, M. Jayachandran," Synthesis and materials properties of transparent conducting In_2O_3 films prepared by sol–gel-spin coating technique", Journal of Physics and Chemistry of Solids, vol. 68, pp. 1380-1389(2007).

[7] A. Bagheri Khatibani , S.M. Rozati and Z. Bargbidi ," Preparation, Study and Nano scale Growth of Indium Oxide Thin Films", ACTA PHYSICA POLONICA A , Vol. 122 , No. 1 (2012).

[8] Joseph Panneerdoss , Johnson Jeyakumar S, Ramalingam S and Jothibas M, "Preparation, Characterization, Spectroscopic (FT-IR, FT-Raman, UV and Visible) Investigation, Optical and Physico Chemical Property Analysis on In2O3 Thin Films", Theoretical & Computational Science, vol. 2 , pp. 1-12, (2015).

[9] S. Marikkannu , M. Kashif , A.Ayeshamariam, V. S. Vidhya , N.Sethupathi ,Shakkthivel Piraman and M.Jayachandran," Studies on jet neuliser pyrolysed indium oxide thin films and its characterizations" Int. J. Nanoelectronics and Materials, vol. 8,pp. 99-110, (2015).

[10] G. Cheng, E. Stern, S. Guthrie, M.A. Reed, R. Klie, Y. Hao, G. Meng, L. Zhang, Appl. Phys. A 85, 233 (2006).

[11] N. Memarian, S.M. Rozati, E. Elamurugu, E. Fortu- nato, J. Phys. Status Solidi C 7, 2277 (2010).

[12] S. Golshahi, S.M. Rozati, R. Martins, E. Fortunato, Thin Solid Films 518, 1149 (2009).

[13] S. Boycheva, A.K. Sytchkova, M.L. Grilli, A. Piegari, Thin Solid Films 515, 8469 (2007).

[14] A. Bagheri khatibani and A. Abdolahzadeh Ziabari, S. M. Rozati and Z. Bargbidi and G. Kiriakidis," Characterization and Gas-sensing Performance of Spray Pyrolysed In_2O_3 Thin Films: Substrate Temperature Effect", Trans. Electr. Electron. Mater. 13(3) 111 (2012): A. Bagheri khatibani et al.

[15] M. Thirumoorthi, J. Thomas Joseph Prakash," Structure, optical and electrical properties of indium tin oxide ultrathin films prepared by jet nebulizer spray pyrolysis technique", Journal of Asian Ceramic Societies 4 124–132 (2016).

[16] C. Kittel, "Introduction to Solid State Physics", (5th Edition) Wiley EasternLtd., New Delhi (1979).

[17] Salam Amir Yousif, Jenan Mohamed Abass," Structural, Morphological and Optical Characterization of SnO_2:F thin films prepared by Chemical spray Pyrolysis", International Letters of Chemistry, Physics and Astronomy, Vol. 18, pp 90-102, (2013).

[18] N.G. Pramod, S.N. Pandey, and P.P. Sahay," Sn-Doped In_2O_3 Nanocrystalline Thin Films Deposited by Spray Pyrolysis: Microstructural, Optical, Electrical, and Formaldehyde-Sensing Characteristics", Journal of Thermal Spray Technology, Vol. 22(6), pp. 1035–1043, August (2013).

[19] Jehan Abdul Sattar Salman, Zainab A. Al-Ramadhan and Hamsa Abdul Karem Hmud," Antibacterial effect and structural properties of PVA-PVP-AGNANO composites ", EUROPEAN JOURNAL OF BIOMEDICAL AND PHARMACEUTICAL SCIENCES, vol. 4, pp. 35-41 ,(2016).

[20] Atheer Ibraheem Abd Ali," Molarities effect on structural and optical properties of ZnO prepared by spray pyrolysis" ,International Journal of Scientific & Engineering Research, Volume 5, Issue 1, January-2014.

[21] Alia A.A.Shehab, Najiba A.AL-Hamadni and Duha M.A.Latif," Effect of annealing temperature on structure properties of SnS thin films" PCAIJ, vol. 9(7), pp. 255-259,(2014).

[22] Hanan Raad Kutif and Ali Ahmed Yousif," Influence Of Structural Properties Of Pure SnO_2,Fe_2O_3 And Nanocomposite SnO_2 /Fe_2O_3 Thin Films Deposited By Spray Pyrolysis Technique", Journal of Multidisciplinary Engineering Science Studies (JMESS) Vol. 2 Issue 10, October (2016).

[23] Harith Ibrahem and Mariam Moghdad ," Preparation of ITO thin film by Sol-Gel method", IPASJ International Journal of Electrical Engineering (IIJEE) , Vol. 1, Issue 6, December (2013).

[24] Ali H. Al-hamdani,"Structural and Optoelectronic Properties of Nanostructured ITO Thin Films Deposited by Chemical Spray Pyrolysis Technique", Journal of Materials Science and Engineering(DAVID PUBLISHING) B 4 (12), pp. 346-352, (2014).

[25] V R Viji , K S Kumar , M mary Stella and Vaidyanh ,"Studies on the properties of dip-coated indium tin oxide films considering substrate vibration ", Indian Journal of pure & Applied Physics vol 43 pp 368-371 (2005).

[26] Nabeel A. Bakr , Sabah A. Salman and Mohammed N. Ali ," Effect of Fluorine Doping on Structural and Optical Properties of SnO_2 Thin Films Prepared by Chemical Spray Pyrolysis Method", Advances in Materials 5(4): 23-30 (2016).

[27] Dr. Saryia D.M AL-Algawi, Dr. SelmaM.H Al-Jawad and Noor M. Saadoon,"Physical Properties of Indium Tin Oxide (ITO) Nanopartical Thin Films Used as Gas Sensor", Eng. &Tech.Journal, Vol. 33,Part (B), No.1 (2015).

[28] Y. Caglar, S. Ilican and M. Caglar," Single-oscillator model and determination of optical constantsof spray pyrolyzed amorphous SnO2 thin films", Eur. Phys. J. B 58, pp. 251-256 (2007).